

Bioreactor Design Studies for a Hydrogen-Producing Bacterium

EDWARD J. WOLFRUM* AND ANDREW S. WATT

National Renewable Energy Laboratory,
1617 Cole Boulevard, Golden, CO 80401,
E-mail: ed_wolfrum@nrel.gov

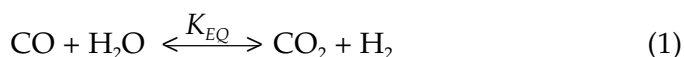
Abstract

Carbon monoxide (CO) can be metabolized by a number of microorganisms along with water to produce hydrogen (H₂) and carbon dioxide. National Renewable Energy Laboratory researchers have isolated a number of bacteria that perform this so-called water-gas shift reaction at ambient temperatures. We performed experiments to measure the rate of CO conversion and H₂ production in a trickle-bed reactor (TBR). The liquid recirculation rate and the reactor support material both affected the mass transfer coefficient, which controls the overall performance of the reactor. A simple reactor model taken from the literature was used to quantitatively compare the performance of the TBR geometry at two different size scales. Good agreement between the two reactor scales was obtained.

Index Entries: Synthesis gas; water-gas shift; mass transfer; *Rubrivivax gelatinosus*; hydrogen; carbon monoxide.

Introduction

The biologically mediated water-gas shift reaction may be a cost-effective technology for the conditioning of synthesis gas for storage or direct use within a hydrogen (H₂) fuel cell, where the presence of even low concentrations of carbon monoxide (CO) is deleterious. National Renewable Energy Laboratory (NREL) researchers have isolated a number of photosynthetic bacteria that perform the water-gas shift reaction, in which CO is oxidized to carbon dioxide (CO₂) while water is simultaneously reduced to hydrogen. The overall stoichiometry of this reversible reaction is as follows:



*Author to whom all correspondence and reprint requests should be addressed.

One significant advantage of using bacteria to perform the water-gas shift reaction is their ability to operate at ambient temperature, where the reaction is not equilibrium limited (at 25°C, $K_{EQ} \sim 5 \times 10^4$ [1]). The advantages of low operating temperature, rapid reaction rate, and lack of equilibrium limitation make the biologic shift reaction a promising alternative to conventional shift technologies.

The ability of bacterial cells to perform the reaction in Eq. 1 is relatively unique, since only a few species have been reported to perform this reaction. This ability was reported by Uffen (2) for *Rhodopseudomonas* sp. (but see later discussion on nomenclature). Dashevicz and Uffen (3) later reported the ability of *Rhodospirillum rubrum* to perform the water-gas shift reaction as well. Bott et al. (4) generated H₂ from CO using the methanogen *Methanosarcina barkeri* when methane formation was inhibited by bromoethanesulfonate. Recent publications report that *Rhodopseudomonas palustris* P4 (5) and *Citrobacter* sp. 19 (6) also perform this reaction.

The evolution of the name *Rubrivivax gelatinosus* is somewhat complicated. Uffen (2) first reported the water-gas shift reaction being performed by a strain of the bacterium *Rhodopseudomonas* isolated from the natural environment. Later he identified this strain as *Rhodopseudomonas gelatinosus* (3). Certain species of "purple nonsulfur" bacteria subsequently were reordered (7), and in later work, Champine and Uffen (8) referred to this species as *Rhodocyclus gelatinosus*. Later, *Rhodocyclus gelatinosus* was reclassified to its present name, *R. gelatinosus* (9).

The main goal of the present work was to compare the performance of two trickle-bed reactors (TBRs) of similar geometry but different sizes, and to examine the effect of liquid recirculation rate on reactor performance. For mass transfer involving sparingly soluble gases, including both CO and O₂, the resistance to mass transfer is in the liquid phase (10). In the case of rapid reaction within the liquid phase, the over-all reactor performance is controlled by the mass transfer rate. In the present work, we developed a model by assuming that the shift rate in a TBR is controlled by the rate of CO transfer from the gas to the liquid phase. We later tested this assumption and found it valid.

A number of researchers have investigated the biologic conversion of gaseous substrates to produce fuels and chemicals. Klasson et al. (11) investigated CO conversion to acetate using the bacterium *Peptostreptococcus productus* in a chemostat, a packed bubble column, and a TBR. They developed a simple reactor model and used it to calculate mass transfer rates for each reactor tested and demonstrated that higher liquid recirculation rates gave higher mass transfer rates in the TBR. They did not determine specific CO uptake rate parameters in this work, since this rate was limited by bulk (gas-liquid) CO mass transfer for all experiments. Kimmel et al. (12) used a triculture of *R. rubrum*, *M. barkeri*, and *Methanobacterium formicicum* to produce methane from synthesis gas using two different size TBRs. *R. rubrum* performed the water-gas shift reaction to produce H₂ and CO₂, and the two methanogens subsequently converted these gases to CH₄. These

investigators compared the performance of the two reactors but got considerably lower conversion rates in the larger column, even though they operated it at slightly higher liquid velocities. They pointed to poor liquid distribution and the possibility of insufficient *R. rubrum* cell concentrations in the larger column as likely causes of the differences between the two reactors. Cowger et al. (13) investigated the water-gas shift reaction using *R. rubrum* in a TBR and a continuous stirred-tank reactor, and demonstrated the effect of liquid recirculation rate on the overall performance of the TBR.

In the present study, we used a monoculture of the photosynthetic bacterium *R. gelatinosus* CBS-2 to carry out the water-gas shift reaction (Eq. 1) in a TBR and used a simple reactor model taken from the literature to analyze its mass transfer characteristics. We examined the influence of reactor support size and liquid recirculation rate on CO conversion in two different reactors of identical geometry but different size. This work thus extends the previous outlined work by more successfully comparing the performance of similar reactor geometries at different scales and examining in more detail the influence of liquid recirculation rate on TBR performance. We also directly compare the results of this work to the results of the aforementioned TBR experiments (11–13) and then explicitly test the assumption of mass transfer limitation.

Materials and Methods

The reactor design used was a TBR, shown schematically in Fig. 1. Both a 1-L and a 5-L TBR assembly were used. The 1-L TBR assembly consisted of a 5.08-cm (nominal) glass pipe 61 cm long. Rubber stoppers (#11 size) were inserted at each end of the glass pipe and acted as end caps. The reactor support (either 3- or 6-mm soda lime glass beads) rested on a stainless steel mesh approx 7.6 cm above the bottom of the reactor. This space provided a sump area where the recirculating liquid collected and could be conveniently sampled for cell density and pH. The gas inlet and outlet fittings that passed through the rubber stopper end caps were 1/8-in.-stainless steel tubing, and the liquid inlet and outlet fittings were 1/4-in.-stainless steel tubing. The inlet fittings (gas and liquid) were located in the center of each end cap, with the corresponding outlet fittings offset slightly. The liquid drained into the reactor sump by gravity and was recirculated using a peristaltic pump and 1/4-in.-flexible tubing (MasterFlex #24 Norprene tubing) back to the top of the TBR. The empty bed volumes of the reactors were 950 and 1100 mL for the 3- and 6mm bead reactors, respectively. The 5-L TBR assembly was conceptually similar to the 1-L assembly except that the reactor was composed of 7.6-cm-diameter glass tubing, the rubber stoppers were larger (#14 size), and gas and liquid inlet and outlet fittings were 1/4-in. stainless steel. It had an empty bed volume of 5.0 L. All reactors were operated at ambient laboratory temperature ($25 \pm 2^\circ\text{C}$). Experiments were performed at ambient pressure, which in Golden, CO, is 0.82 atm.

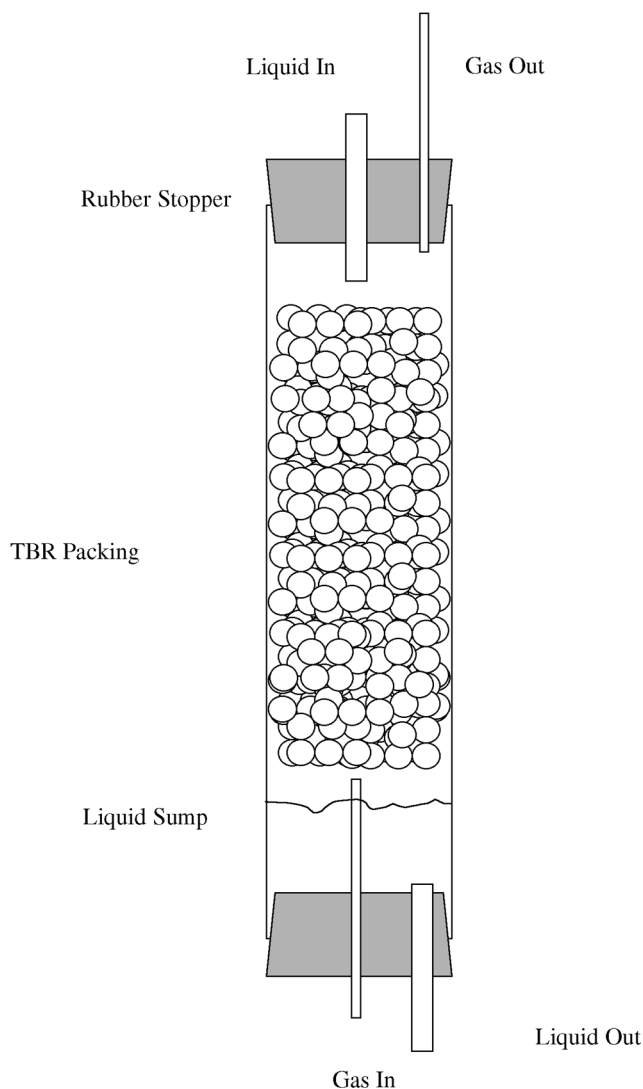


Fig. 1. Schematic diagram of countercurrent TBRs used. The inner diameters of the 1- and 5-L TBR assemblies were 2-3 in. respectively (see text).

The microorganism used was *R. gelatinosus* CBS-2. This purple, nonsulfur photosynthetic bacterium was isolated from the natural environment by the Weaver group at NREL. Previous reports from NREL had classified this specific strain as *Rhodobacter* sp. based on spectral and nutritional properties (14). However, recent 16S rRNA analysis (unpublished results) has permitted a definitive classification as *R. gelatinosus*.

The minimal culture medium (M-1 basal) had the following composition (amounts are for 1 L of final media preparation): basal salts (120 mg of $\text{MgSO}_4 \cdot 7\text{H}_2\text{O}$, 75 mg of $\text{CaCl}_2 \cdot 2\text{H}_2\text{O}$, 11.8 mg of $\text{FeSO}_4 \cdot 7\text{H}_2\text{O}$, 20 mg of EDTA), trace elements (2.8 mg of H_3BO_3 , 1.6 mg of $\text{MnSO}_4 \cdot \text{H}_2\text{O}$, 0.75 mg of

$Na_2MoO_4 \cdot 2H_2O$, 0.24 mg of $ZnSO_4 \cdot 7H_2O$, 0.04 mg of $Cu[NO_3]_2 \cdot 3H_2O$, 0.8 mg of $CoCl_2 \cdot 6H_2O$, 0.8 mg of $NiCl_2 \cdot 6H_2O$, phosphates (1.2 g of KH_2PO_4 , 1.8 g of K_2HPO_4), vitamins (1.0 mg of thiamine HCl, 15 μ g of biotin, 1.0 mg of nicotinic acid, 10 μ g of B_{12} , 0.1 mg of *p*-aminobenzoic acid), and ammonia (1.5 g of NH_4Cl). In addition, malate (5 g/L) and yeast extract (0.5 g/L) were added as carbon sources. The medium was prepared using deionized water and stock solutions of basal salts, trace elements, vitamins, buffers, ammonia, and D,L-malic acid. Yeast extract was added as a powder immediately prior to sterilization. The stock solutions were in turn prepared using stock chemicals from various manufacturers, which were used as received.

Pure cultures of *R. gelatinosus* CBS-2 were grown and periodically subcultured under sterile conditions using 20-mL screw-top test tubes and 200-mL serum flasks. These vessels were kept under incandescent illumination until used to inoculate the TBR assemblies. The microorganisms were not exposed to CO during the growth/subculture process.

The 1-L TBR experiments proceeded as follows. The reactor, including the external liquid recirculation loop, was assembled, autoclave sterilized, and allowed to cool. The assembly was then installed in a canopy hood, and the gas inlet fitting was connected to the source gas (20% CO, 0.5% He as tracer gas, balance N_2). The reactor was then rinsed with sterile M-1 medium while gas flow was initiated. After several reactor volumes of gas were allowed to flow through the reactor, the reactor was drained of any remaining medium and inoculated with one serum flask of *R. gelatinosus* CBS-2. Default gas and liquid flow rates were established (liquid recirculation rate of 200 mL/min, gas flow rate of 25 accm), and the reactor sump was illuminated with a 65-W incandescent lamp for several days. CO uptake (and concomitant H_2 production) was induced within approx 48 h. Once H_2 production reached steady state, the lamp was turned off and the reactor loosely covered with black cloth. The operating conditions of the reactor (gas and liquid flow rates) were periodically adjusted, and the outlet gas composition was monitored over time, using a portable gas chromatograph (Agilent P200). The reactor typically required 12 h or more to reach steady-state after a change in operating conditions. These steady state values were recorded over the course of several hours, and then the operating conditions were changed. The total liquid volume in the reactors (including the reactor sump) was approx 200 mL. There was some liquid loss owing to evaporation and pH/OD sampling. Periodically, ~20-mL aliquots of sterile M-1 medium were added to the reactor to replenish the liquid. No effect on reactor productivity (CO shift rate) was seen as a result of these additions to the medium.

The 5-L TBR experiments proceeded in a similar fashion, except that the reactor was not autoclaved. Rather, it was washed with standard laboratory detergent (Alconox) and rinsed thoroughly with deionized water passed through a sterile 0.2- μ m filter. Larger liquid inocula were used, typically 600 mL. The default gas and liquid flow rates for the 5-L TBR assembly were 65 accm and 500 mL/min, respectively.

As mentioned earlier, the inlet gas stream contained 0.5% He as an inert tracer to compensate for changes in the volumetric gas flow rate across the reactor. The water-gas shift reaction causes an increase in the volumetric gas flow rate, since 2 mol of gas (H_2 , CO_2) are produced for every mole of CO consumed (water is supplied by the medium). This change in volume would bias CO outlet concentrations low, since CO would not only be consumed by the microorganisms but also diluted by additional gas flow. Similarly, outlet H_2 concentrations would be biased low owing to dilution. Since He is neither consumed nor produced in the reaction, its molar flow rate is constant. Thus, any change in He concentration must correspond to a change in the overall gas flow rate. This correction factor was applied to all outlet concentration measurements.

The performance of the TBR reactor assembly can be modeled as a simple plug-flow reactor, with the overall reaction rate controlled by a mass transfer coefficient. This model was developed by researchers at the University of Arkansas for several different reactor geometries, including packed bubble column reactors and TBRs (11,15,16). When the reaction rate is limited by the rate of mass transfer, the steady-state liquid concentration of reactant (in this case, CO) can be assumed to be zero, and the controlling equation for an ideal TBR is

$$v_z \frac{dC}{dz} = -\frac{k_L a}{H} C \quad (2)$$

in which v_z is the superficial gas velocity; C is the gas-phase concentration of reactant; $k_L a$ is the overall mass transfer coefficient (based on empty bed reactor volume); and H is the Henry's Law coefficient of the reactant, a measure of its solubility in the liquid phase. Often, the mass transfer coefficient is based on the liquid holdup volume, and the term $k_L a$ in the Eq. 2 is replaced by $k_L a \cdot \epsilon_L$, in which ϵ_L is the liquid porosity (the ratio of the liquid holdup volume to the empty bed reactor volume). In this work, we base the mass transfer coefficient on the empty bed reactor volume. This equation can be easily integrated to yield

$$C_o = C_i \exp\left(-\frac{k_L a}{H} t_{EBCT}\right) \quad (3)$$

in which C_o and C_i are the outlet and inlet reactant concentrations, respectively; and t_{EBCT} is the empty bed contact time (EBCT) of the reactant in the reactor, calculated as the empty bed volume of the reactor divided by the volumetric gas flow rate (measured at the inlet of the reactor). The EBCT is therefore equivalent to the "space time" or "mean residence time" of the reactor (17) and represents the time required to treat 1 vol of gas equal to the overall reactor volume at the inlet temperature and pressure. By using an overall mass transfer coefficient in Eqs. 2 and 3, we treat the reactor system as a "black box," a view reinforced by the use of t_{EBCT} as the independent variable. Thus, reactors with variable geometries, volumes, and support materials can be directly compared using this equation.

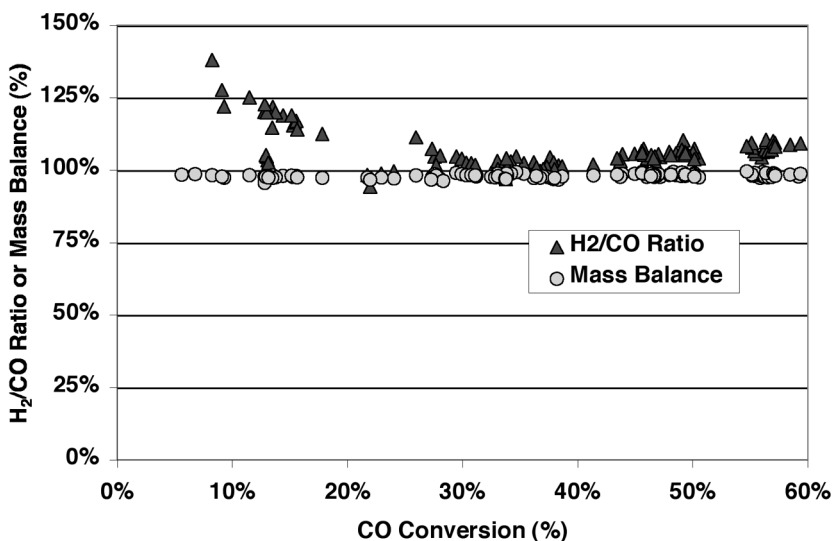


Fig. 2. Effect of CO conversion on overall mass balance and H_2 :CO ratio in outlet gas stream in 1-L TBR assembly. The liquid recirculation rate was 200 mL/min and the gas flow rate was 25 accm.

The change in the volumetric flow rate of the reactant gas owing to the water-gas shift reaction causes the actual residence time of a CO molecule within the reactor to vary with conversion. However, such variations are small. The maximum CO conversion reported in this work is 74%, so the maximum volume change of the 20% CO feed stream would correspond to a 15% change in volumetric flow at the exit. This corresponds to an 8% volume-averaged increase in flow across the reactor, which, in turn, represents a decrease of 8% in the actual contact time. The model presented in Eq. 3 does not consider these changes, and the data are presented in terms of EBCT as defined earlier.

Results and Discussion

Figure 2 shows how the measured mass balance and the ratio of H_2 produced to CO consumed, $H_2/(CO_{in}-CO_{out})$, vary with CO conversion. The mass balance data (defined as the sum of concentrations of all species in the outlet stream: CO, CO_2 , H_2 , N_2 , He) were very stable at $98.0 \pm 0.8\%$ over the entire course of the experiment, which lasted 15 d. This suggests that the calibration of the gas chromatograph was stable over the course of the experiment. The H_2 :CO ratio was not as stable: $107 \pm 7\%$. This ratio appears highest at lower conversions, which we believe is an artifact of the analytical method. At lower conversions, the CO conversion was difficult to measure precisely (10% conversion of a 20% CO stream causes a 2% change in absolute concentration) and is likely underestimated, leading to higher H_2 :CO ratios (we have subsequently improved our analytical

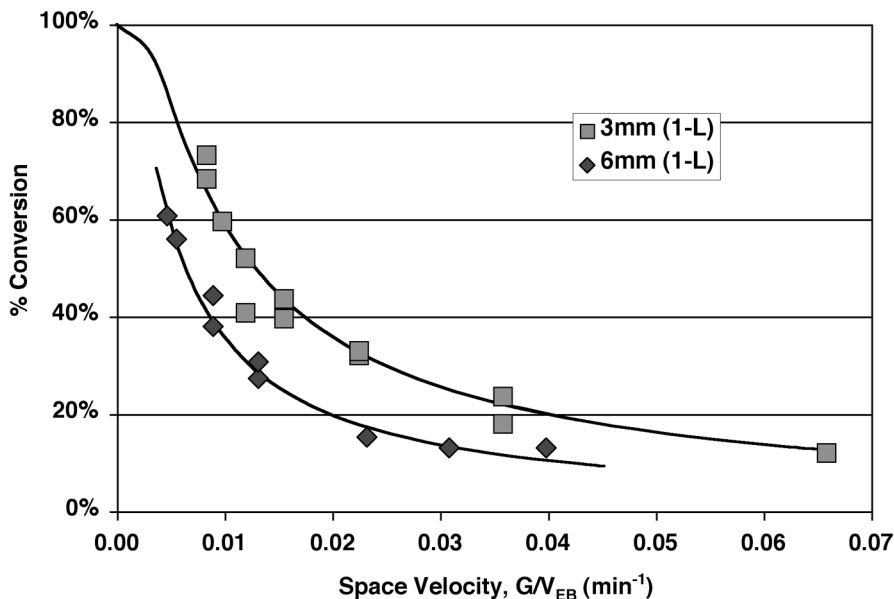


Fig. 3. Comparison of CO conversion vs space velocity in 1-L TBR assembly using nonporous glass bead supports of two different sizes. The liquid recirculation rate was 200 mL/min. The small-diameter reactor support provides higher conversion efficiencies at a given space velocity.

instrumentation, and this artifact has disappeared). Nonetheless, the H_2 :CO ratio is approximately unity for most of the experiment, which is in agreement with theoretical stoichiometry.

Figure 3 shows the effect of the size of a nonporous glass bead reactor support on CO conversion in the 1-L TBR assembly. The abscissa is the space velocity, which is the ratio of the volumetric inlet gas flow rate to the empty bed reactor volume. It is the inverse of the EBCT. The smaller diameter support (3 mm) clearly gives better performance at the same superficial liquid velocity. Equation 3 can be linearized by rearranging terms and then taking the natural logarithms to give

$$\ln \frac{C_o}{C_i} = \frac{k_L a}{H} t_{\text{EBCT}} \quad (4)$$

The data in Fig. 3 are replotted according to Eq. 4 in Fig. 4. The slopes of the solid lines represent the quantity $k_L a/H$ (the intercepts of the linear curve fits are not significantly different from zero at the 95% confidence level). Since the Henry's Law coefficient for CO (at 25°C) is 57,800 atm (mol fraction)⁻¹ or 42.3 (unitless) (18), the overall mass transfer coefficients for the small and large supports, based on total reactor volume according to Eqs. 2 and 3, have values of 0.42 and 0.19 min^{-1} , respectively.

The ability of this simple model to predict reactor performance at different scales is tested in Figs. 5 and 6, in which the influence of the same

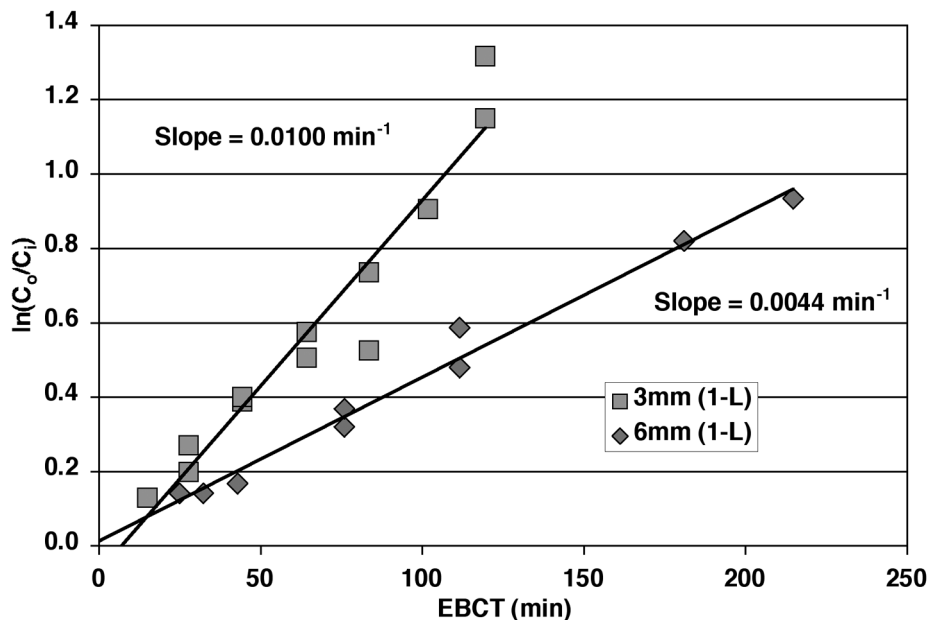


Fig. 4. $\ln(C_o/C_i)$ vs EBCT for 1-L TBR experiments with two different size supports. The liquid recirculation rate was 200 mL/min. The slopes of the regression line provide an estimate of the overall mass transfer coefficient in the system. The intercepts are not significantly different from zero at the 95% confidence level.

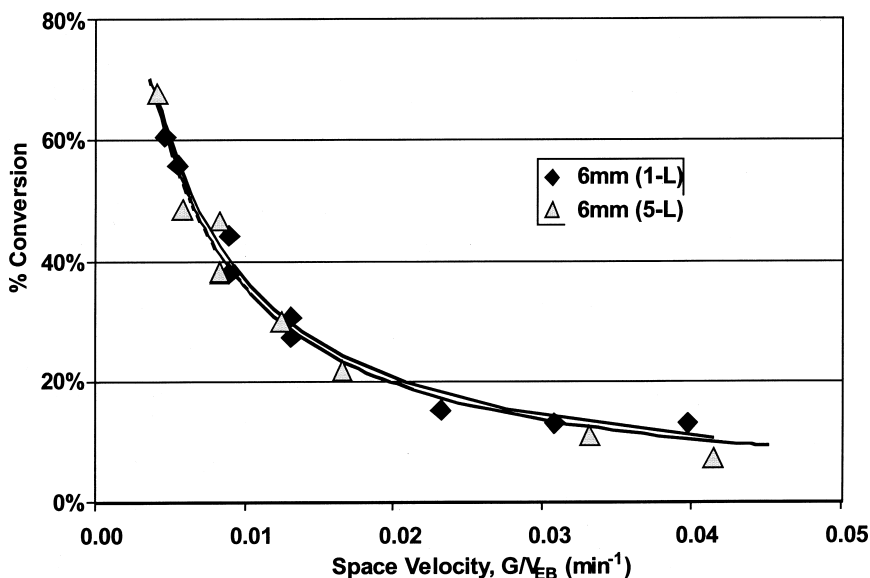


Fig. 5. Comparison of CO conversion vs space velocity using 6-mm-diameter glass bead support in 1- and 5-L TBR assemblies. The liquid recirculation rate was 200 mL/min for the 1-L TBR and 500 mL/min for the 5-L TBR, yielding superficial liquid velocities of 9.89 and 10.96 cm/min, respectively.

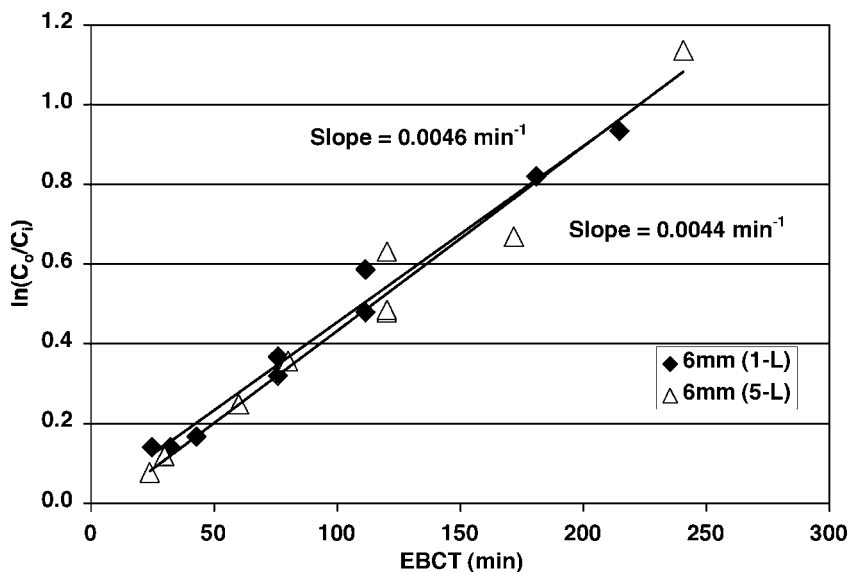


Fig. 6. $\ln(C_0/C_1)$ vs EBCT for 6-mm-diameter glass bead support in 1- and 5-L TBR assemblies. The superficial liquid velocities were 9.89 and 10.96 cm/min in the 1- and 5-L TBR assemblies, respectively. The slopes of the regression lines provide an estimate of the overall mass transfer coefficient in the system. The intercepts are not significantly different from zero at the 95% confidence level.

reactor support in the 1- and 5-L TBR assemblies is compared according to Eqs. 3 and 4, respectively. The performance of the two reactors is essentially identical (again, the intercept of the 5-L reactor data curve fit in Fig. 6 is not statistically significantly different from zero at the 95% confidence level). Note that the superficial liquid-phase velocities in the two reactors are slightly different: 1.06 and 1.18 cm/s in the 1- and 5-L TBR assemblies, respectively. Since the liquid velocity in the 5-L reactor is slightly higher, we would expect slightly better performance in this reactor, although the data of Figs. 5 and 6 do not show this trend. Nonetheless, the close agreement in reactor performance at the two different scales give us confidence in our understanding of the reactor dynamics, and in our ability to predict accurately the performance of larger reactors from the performance of smaller ones.

Increasing the liquid recirculation rate increases the performance of both reactors, as shown in Fig. 7. The abscissa is the superficial liquid velocity, which is the volumetric flow rate of the liquid phase divided by the cross-sectional area of the reactor (19). Two important features of the data in Fig. 7 are worth noting. First, the slopes of the curve fit lines are slightly different (at the 95% confidence level), with the two data sets intersecting at a superficial liquid velocity of approx 11 cm/s. Second, both curve fit lines appear to have nonzero intercepts.

The different slopes of the curve-fit lines for the 1- and 5-L reactors indicate that the reactors are not behaving identically, although the over-

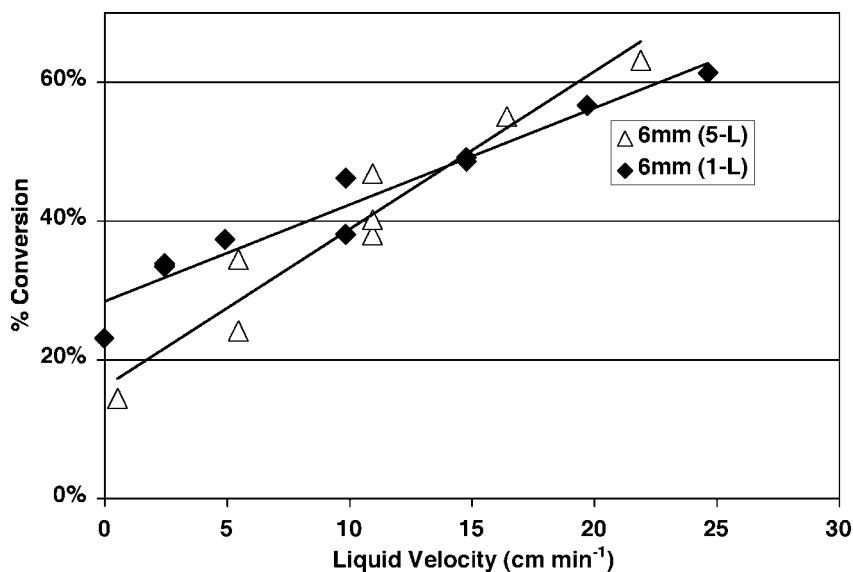


Fig. 7. Effect of liquid flow rate on conversion for 6-mm-diameter glass bead support in 1- and 5-L TBR assemblies. Increased liquid flow rate provided increased overall mass transfer coefficients in both TBR assemblies, although the rates of increase are slightly different.

all trends of both data sets, increasing mass transfer rates at increasing superficial liquid velocities, are in agreement. The intersection of the two data sets occurs at approx 11 cm/s, the superficial velocity used for the experiments in which the feed gas flow rate was varied. Thus, the very close agreement in reactor performance between the 1- and 5-L reactors (Figs. 5 and 6) is owing at least in part to the fact that their default liquid recirculation rates resulted in such close agreement in CO conversion. If the experiments that produced the data in Fig. 5 were repeated at a different recirculation rate, it is possible that the agreement between the two curves would not be as close.

The nonzero shift activity at zero liquid flow indicates either nonbiologic shift activity or the presence of bacteria in the reactor in the absence of liquid recirculation. Control experiments (data not shown) clearly indicate that no nonbiologic shift activity exists in the system. The supports used in this work were nonporous glass spheres, which should not provide an attractive surface for the growth of bacteria. However, a small amount of liquid holdup was noticed in the 1-L reactor at zero liquid velocity. Whether the shift activity was owing to the presence of bacteria suspended in medium that did not drain from the reactor, or whether it was owing to immobilized bacteria (biofilm) is not known. However, this issue, although troubling, does not invalidate the comparison of reactor scales in Figs. 5 and 6, since those experiments were performed at a nonzero liquid recirculation rate.

The studies by Klasson et al. (11), Kimmel et al. (12), and Cowger et al. (13) provide experimental results for the fermentation of CO in TBRs, and, thus, it is appropriate to compare the results of the present work to those studies. In the cited studies and ours, the overall reaction rates are controlled not by intrinsic microbial productivities but by mass transfer. Table 1 summarizes the results of our study and the three cited studies, and shows two different parameters that can be used to characterize the overall performance of a TBR: the overall mass transfer coefficient, $k_L a$, and the overall rate constant, k_{app} ; the two are related through the Henry's Law coefficient, H :

$$k_{app} = \frac{k_L a}{H} \quad (5)$$

Note that both parameters are based on the empty bed volume of the reactor, and that while the overall rate constant, k_{app} , has units of inverse time, the selection of units for the Henry's Law coefficient, H , controls the units of the overall mass transfer parameter, $k_L a$. In Table 1, we use a dimensionless form of H , so both parameters have identical units.

Several observations can be made regarding the data in Table 1. The specific support used affects the measured mass transfer rates. At a given value of superficial liquid velocity, V_L , Intalox saddles provide higher mass transfer rates than do solid spheres. We found $k_L a$ values of 0.19 and 0.42 min^{-1} for 6- and 3-mm beads, respectively at $V_L = 9.9$ cm/min, while Cowger et al. (13) reported $k_L a$ values of 0.37 min^{-1} at $V_L = 5.0$ for saddles. When they increased V_L to 12 cm/min, they measured a $k_L a$ value of 0.63 min^{-1} . Klasson et al. (11) reported similar results. Note that we, Cowger et al. (13), and Klasson et al. (11) used reactors of approx 1-L volumes.

Kimmel et al. (12) investigated the performance of the two reactor sizes, which differed in volume by a factor of approx 25. The measured performance of the two reactors was significantly different: the smaller reactor had an overall k_{app} value eight times larger than the larger reactor. Note that they did not report a $k_L a$ for the larger reactor, and they specifically point out that the larger reactor was not operating under mass transfer-limiting conditions. Our results, although at a more modest scale-up volume ratio of approx 5, indicate essentially identical performance at the two scales.

As mentioned in Kimmel et al. (12), Charpentier (20) recommends a value of $k_L a = 0.008 \text{ s}^{-1} = 0.48 \text{ min}^{-1}$ for gas-liquid reactors under trickle flow conditions with packing diameters >2 mm, although this approximation shows no dependence on gas or liquid flow rates. All the data in Table 1 are in general agreement with this value. This recommended value must be taken as an approximation, since the mass transfer coefficient should be a function of the hydrodynamic conditions of the column in question. For the case of gas-liquid mass transfer of sparingly soluble gases, the overall mass transfer rate is controlled by liquid side resistance (10). In such a case, only

Table 1
Summary of Mass Transfer Coefficients for CO Conversion in Trickle-Bed Reactors

Reference	Reactor volume (L)	Reactor packing	Parameter reported	Reported value	Units	k_{app} (min ⁻¹) ^a	$k_L a$ (min ⁻¹) ^a	Superficial liquid velocity (V_L) (cm/min)
11	1.1	1/4-in. Intalox saddles	$K_L a \cdot \epsilon_L / H$	30.3	mmol L ⁻¹	0.0123	0.52	19.3
				16.2	atm ⁻¹ h ⁻¹	0.0066	0.28	15.0
				8.7		0.0035	0.15	6.1
12	1.1	1/4-in. Intalox saddles	$K_L a \cdot \epsilon_L$	53	h ⁻¹	0.0210	0.88	6.1 and 11.2
	26.0	16-mm pall rings and 1/2-in. Intalox saddles	Line (Fig. 5)	—	—	0.0025 ^b	—	6.2
13	1.1	1/4-in. Intalox saddles	$K_L a \cdot \epsilon_L$	22	h ⁻¹	0.0087	0.37	5.0
				38		0.0150	0.63	12.0
This work	0.95	3-mm spheres	k_{app}	0.0100	min ⁻¹	0.0100	0.42	9.9
	1.1	6-mm spheres		0.0044		0.0044	0.19	9.9
	5.0	6-mm spheres		0.0045		0.0045	0.19	11.0

^aThe parameter k_{app} is the apparent first-order rate constant, while the parameter $k_L a$ is the overall liquid-side mass transfer coefficient, both based on the empty-bed reactor volume. They differ in magnitude by the factor 42.3, which is the unitless form of the Henry's Law coefficient for CO, H_{CO} . Other equivalent values of H_{CO} are 57,800 atm (mol fraction)⁻¹ and 1034 L/(atm·mol) (see text).

^bEstimated from the data in Fig. 5 of this reference. The authors do not report a mass transfer coefficient because mass transfer limiting conditions were not reached in this reactor.

the liquid side velocities affect mass transfer. Increasing these velocities can increase the conversion rate (as indicated for our system in Fig. 7), at the expense of greater pumping requirements and the possibility of flooding the column, where the liquid cannot drain through the reactor by gravity fast enough to keep up with the rate of liquid introduced at the top of the TBR.

The development of the model and the interpretation of the results assumed that the reaction was mass transfer limited. To determine this possibility unambiguously, it is necessary to know the specific activity of the microorganism being used. We have performed batch experiments in agitated jars (which we believe to be free of mass transfer limitations) to measure the specific productivity of *R. gelatinosus* CBS-2. Using a 20% CO headspace, we have calculated a specific hydrogen production rate of approx 1.0 mmol/(min·g of cells) at room temperature (unpublished data). We believe this to be a relatively high value. Jung et al. reported H₂ shift rates of 0.35 and 0.50 mmol/(g·min) for *R. palustris* P4 (5) and *Citrobacter* Y19 (6). Klasson et al. (21) reported specific H₂ production rates for *R. rubrum* between 0.067 and 0.15 mmol/(g·min), and calculated a rate expression for specific CO uptake. They also reviewed previous specific rate data reported in the literature, which ranged from 0.04 to 0.17 mmol of H₂/(g·min).

We can determine the extent to which the TBRs we used are mass transfer limited by comparing the specific rate of 1.0 mmol/(min·g of cells) reported previously to the "apparent" specific rate data, defined as the molar rate of H₂ production in the reactor divided by the cell mass in the reactor. The former number can be calculated from the data in Fig. 2, while the latter number is the cell density of the reactor multiplied by the holdup volume (assuming no formation of biofilm). The 3-mm bead reactor had an average cell density of 1.35 g/L, while the 6-mm bead reactor had an average cell density of 1.65 g/L. The holdup volumes at the default recirculation rates of 200 mL/min were 58 and 52 mL for the 3- and 6-mm reactors, respectively. The "apparent specific rate" varied between 0.31 and 0.55 mmol/(min·g of cells) for the 3-mm bead reactor and between 0.21 and 0.45 mmol/(min·g of cells) for the 6-mm bead reactor. Since the "true" specific rate, in the absence of mass transfer limitations, is estimated to be 1.0 mmol/(min·g of cells), we can conclude that the reactors were operating under mass transfer-limiting conditions.

Conclusion

A TBR was used to examine the influence of reactor support size and liquid recirculation rate on the conversion of CO to H₂ by a photosynthetic bacterium. Both reactor parameters affected the mass transfer coefficient, which, in turn, controlled the overall reactor performance. A simple reactor model taken from the literature was used to compare quantitatively the performance of the reactors of identical geometry but different size. Thus, the model can be used to predict the performance of larger reactors based on the performance of smaller ones. The values of the mass transfer coef-

ficients we calculated are in reasonable agreement with those of similar work in the literature.

Acknowledgments

We wish to acknowledge Pin-Ching Maness and Paul F. Weaver of the NREL Basic Sciences Center, who provided guidance and advice throughout the course of this work. Christopher Doelling performed a number of preliminary experiments.

References

1. Bale, C. W., Pelton, A. D., and Thompson, W. T. (2001), *FACT-SAGE*, vol. 5, Ecole Polytechnique de Montreal, Montreal, Canada.
2. Uffen, R. L. (1976), *Proc. Nat. Acad. Sci. USA* **73**(9), 3298–3302.
3. Dashekvicz, M. P. and Uffen, R. L. (1979), *Int. J. Syst. Bacteriol.* **29**(2), 145–148.
4. Bott, M., Eikmanns, B., and Thauer, R. K. (1986) *Eur. J. Biochem.* **159**, 393–98.
5. Jung, G. Y., Jung, H. O., Kim, J. R., et al. (1999), *Biotechnol. Lett.* **21**, 525–529.
6. Jung, G. Y., Kim, J. R., Jung, H. O., et al. (1999), *Biotechnol. Lett.* **21**, 89–873.
7. Imhoff, J. F., Truper, H. G., and Pfennig, N. (1984), *Int. J. Syst. Bacteriol.* **34**, 340–343.
8. Champine, J. E. and Uffen, R. L. (1987), *FEMS Microbiol. Lett.* **44**, 307–311.
9. Willems, A., Gillis, M., and de Ley, J. (1991), *Int. J. Syst. Bacteriol.* **41**, 65–73.
10. Bailey, J. E. and Ollis, D. F. (1977), *Biochemical Engineering Fundamentals*, McGraw-Hill, NY.
11. Klasson, K. T., Elmore, B. B., Vega, J. L., et al. (1990), *Appl. Biochem. Biotechnol.* **24/25**, 857–873.
12. Kimmel, D. E., Klasson, K. T., Clausen, E. C., et al. (1991), *Appl. Biochem. Biotechnol.* **28/29**, 457–469.
13. Cowger, J. P., Klasson, K. T., Ackerson, M. D., et al. (1992), *Appl. Biochem. Biotechnol.* **34/35**, 613–624.
14. Maness, P. C. and Weaver, P. F. (1994), *Appl. Biochem. Biotechnol.* **45,46**, 395–406.
15. Vega, J. L., Clausen, E. C., and Gaddy, J. L. (1989), *Biotechnol. Bioeng.* **34**, 774–784.
16. Vega, J. L., Antorrena, G. M., Clausen, E. C., et al. (1989), *Biotechnol. Bioeng.* **34**, 785–793.
17. Fogler, H. S. (1992), *Elements of Chemical Reactor Engineering*, 2nd ed., Prentice Hall PTR, Upper Saddle River, NJ.
18. Foust, A.S., Wenzel, L. A., Clump, C. W., et al. (1980), *Principles of Unit Operations*, 2nd ed., John Wiley & Sons, NY.
19. Nauman, E. B. (1987), *Chemical Reactor Design*, John Wiley & Sons, NY.
20. Charpentier, J.-C. *Adv. Chem. Eng.* **11**, 1–133.
21. Klasson, K. T., Lundback, K. M. O., Clausen, E. C., et al. (1993), *J. Biotechnol.* **29**, 177–188.



Permission to Use Copyrighted Material

Yes I give the National Renewable Energy Laboratory (NREL) of Golden, Colorado, irrevocable permission to post the following onto its site on the World Wide Web

No

Name of Document, Report, Article, etc.: Bioreactor Design Studies for a Hydrogen-Producing Bacterium. Wolfrum et al. p. 611 of 23rd Symposium on Biotechnology for Fuels and Chemicals, Breckenridge, Colorado, May 2001.

Yes In addition to posting on the Web, I give NREL permission to distribute hard copies of the document through its National Alternative Fuels Hotline in response to requests.

No

When posting on the Web, NREL will credit the copyright holder thus: "Posted on this site with permission from Humana Press." When distributing hard copies, NREL will label the document "Reprinted with permission from Humana Press."

I deny permission to post the document on the Web or to distribute hard copies, but give permission for the document to be abstracted and cited in NREL's database, along with information about obtaining the document directly from the copyright holder. The document can be obtained by writing:

I represent and warrant that I have the full right and authority to grant the rights herein granted and that no one else's permission is required.

Printed name	<i>Thomas B. Langston</i>	Title and company	
Signed name	<i>Thomas B. Langston</i>	Date	<i>4/3/02</i>